

# The Effect of the Half-Width of the 22-GHz Water Vapor Line on Retrievals of Temperature and Water Vapor Profiles with a Twelve-Channel Microwave Radiometer

James C. Liljegren, Sid A. Boukabara, Karen Cady-Pereira, and Shepard A. Clough

**Abstract**—We show that observed biases in retrievals of temperature and water vapor profiles from a twelve-channel microwave radiometer arise from systematic differences between the observed and model-calculated brightness temperatures at five measurement frequencies between 22 and 30 GHz. Replacing the value for the air-broadened half-width of the 22-GHz water vapor line used in the Rosenkranz absorption model with the 5% smaller half-width from the HITRAN compilation largely eliminated the systematic differences in brightness temperatures.

An *a priori* statistical retrieval based on the revised model demonstrated significant improvements in the accuracy and vertical resolution of the retrieved temperature and water vapor profiles. Additional improvements were demonstrated by combining the MWRP retrievals with those from the GOES-8 sounder and by incorporating brightness temperature measurements at off-zenith angles in the retrievals.

**Index Terms**—Microwave remote sensing, spectroscopy, thermodynamic profile retrieval, water vapor absorption.

## I. INTRODUCTION

THE Atmospheric Radiation Measurement (ARM) Program has operated a twelve-channel microwave radiometer profiler (MWRP) [1] since February 2000 at its Southern Great Plains (SGP) site near Lamont, OK.

The MWRP provides real-time vertical profiles of temperature, water vapor, and limited-resolution cloud liquid water from the surface to 10 km in nearly all weather conditions, at approximately 5-min intervals. In contrast to radiosondes, the MWRP provides substantially improved temporal resolution but coarser vertical resolution that declines in proportion to the height above ground level. In this regard, the MWRP data may be more appropriate inputs to numerical weather, climate, and cloud models, which have

Manuscript received May 13, 2004; revised June xx, 2004. This work was supported by the Climate Change Research Division, U. S. Department of Energy, Office of Science, Office of Biological and Environmental Research, under contract W-31-109-Eng-38, as part of the Atmospheric Radiation Measurement Program. Argonne National Laboratory is operated by the University of Chicago for the U. S. Department of Energy.

J. C. Liljegren is with Argonne National Laboratory, Argonne, IL 60439 USA (phone: 630-252-9540; fax: 630-252-9792; e-mail: jcliljegren@anl.gov).

S. A. Boukabara, K. Cady-Pereira, and S. A. Clough are with Atmospheric and Environmental Research (AER), Inc., Lexington, MA.

time steps ranging from 10 s to 30 min but only 20-50 vertical levels [2]. Modelers generally reduce the vertical resolution of the soundings by averaging over the vertical layers of the model.

In evaluating the MWRP for the ARM Program, Liljegren [3] observed significant biases, in comparison with radiosonde data, in the water vapor and temperature profiles retrieved from the MWRP with the artificial neural network algorithms supplied by the manufacturer [4], which were based on the Rosenkranz absorption model [5]. This finding is in agreement with the previous results of Gueldner and Spaenkuch [6].

## II. REVISED ABSORPTION MODEL

We compared brightness temperatures measured in the five K-band channels (22.235, 23.035, 23.835, 26.235, and 30.0 GHz) that span the water vapor resonance centered at 22.235 GHz with calculations based on the absorption model of Rosenkranz [5] with recent modifications [7] (hereinafter R03). To ensure that any dry bias in the radiosondes used in the R03 model calculations did not affect the brightness temperature comparison, ARM's scaled radiosonde product (sgplssondeC1.c1) was used. In this product the relative humidity of the radiosonde is scaled linearly, so that the integrated precipitable water vapor (PWV) matches the PWV derived from a collocated two-channel microwave radiometer (MWR) that measures brightness temperatures at 23.8 and 31.4 GHz. In addition, using the scaled soundings substantially reduces the variability in the model calculations arising from the variability in the radiosonde humidity calibrations.

Prior to April 2002, the retrieval used by ARM to obtain PWV from the MWR brightness temperatures for scaling the radiosondes was based on the Liebe and Layton [8] absorption model. After April 2002 the retrieval – and sonde scaling – was based on [5], which yielded 2% larger values of PWV. For this study we have rescaled the radiosondes from the period after April 2002 to be consistent with [8].

Because radiosondes do not measure cloud liquid water amount, the comparisons were limited to liquid-water-cloud-free conditions by requiring that the magnitude of the retrieved liquid water path (LWP) was less than 50 g/m<sup>2</sup> (the expected

root-mean-square error in the LWP retrieval) and the sky temperature measured with a collocated 10- $\mu$ m infrared pyrometer was less than  $-15$  °C.

The model calculations were performed only for the center frequency of the MWRP measurement channels and do not account for the radiometer band pass, which extends from 40–190 MHz on either side of the center frequency. We investigated the effect of the band pass by calculating the brightness temperature at 10 MHz intervals over the band pass and then comparing the average with the value for the center frequency alone. At 22.235 GHz we found that the average brightness temperature was less than the center frequency value by only 0.11 K (PWV = 1 cm), to 0.27 K (PWV = 4 cm). The differences at the other frequencies were smaller.

The results of the comparisons, presented in Fig. 1 and summarized in Table 1, show that for the unmodified Rosenkranz model the slope of the measured–modeled brightness temperature differences is large at 22.235 GHz and that the slope of the differences declines with increasing frequency separation from the line center, suggesting a dependence on line shape (through the half-width) rather than a line strength dependence. Moreover, the strength of the 22.235 GHz water vapor line has been quite accurately determined in the laboratory from Stark Effect measurements of the dipole moment [9], whereas the half-width is less

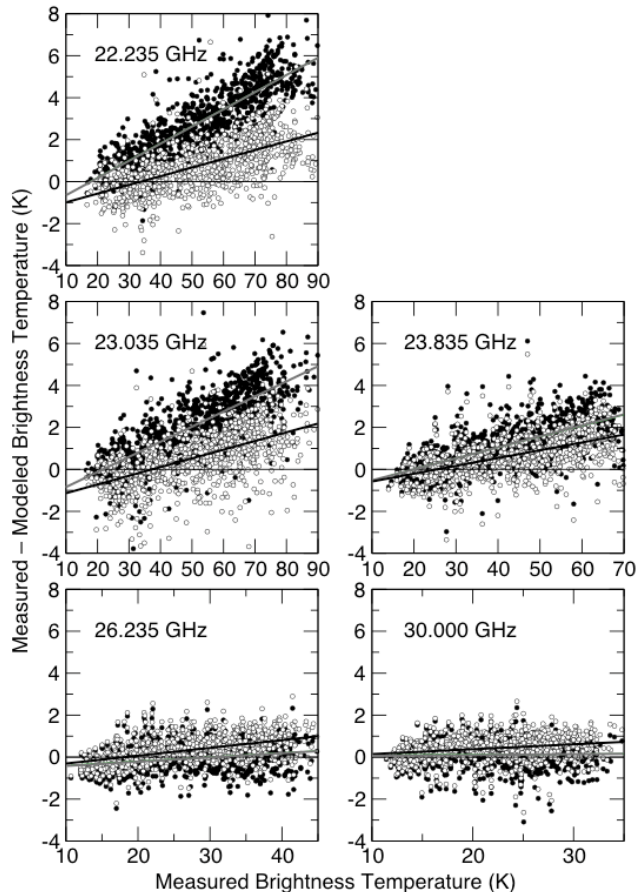


Fig.1. Differences between measured and model-calculated brightness temperatures for the half-width of the 22-GHz absorption line from Liebe and Dillon [10] (solid circles, gray regression line) and the half-width from HITRAN [11] (open circles, black regression line) for liquid-water-cloud-free conditions.

TABLE I  
SLOPES OF  $\Delta T_B$  VS.  $T_B$  REGRESSION LINES IN FIG. 1 (K/K)

Model	22.235 GHz	23.035 GHz	23.835 GHz	26.235 GHz	30.0 GHz
R03	0.082	0.073	0.052	0.020	0.003
R03-H	0.042	0.042	0.038	0.037	0.024

certain.

The air-broadened half-width used by Rosenkranz [10] is 0.00281 GHz/kPa at 300 K, whereas the value from the HITRAN database [11], adjusted to 300 K, is 0.002656 GHz/kPa, which is about 5% less. (Because HITRAN does not list a self-broadened half-width for this line, a value 4.8 times the air-broadened half-width was used [5].) When the HITRAN value for the half-width was substituted in the calculations (hereinafter R03-H), the agreement with the measured brightness temperatures improved dramatically, as shown in Fig. 1, and the slopes of the differences are nearly independent of frequency.

The results in Fig. 1 are dependent on the absorption model underlying the PWV retrieval used to scale the radiosondes. To investigate the effect of this dependence on our results, the radiosondes were rescaled to increase their PWV by 2%, consistent with [5], and the comparison between measurements and R03 model calculations was repeated. The results, summarized in Table 2, reveal that a 2% PWV increase reduces the brightness temperature differences 1.5%–2.4% (i.e., the slopes are reduced 0.015 K/K – 0.024 K/K). The increasing reduction in the slope with frequency is influenced by the water vapor continuum. The trend of decreasing slope with frequency persists; in fact the slope at 30 GHz has become negative. Increasing PWV (or line strength) will not produce simultaneous agreement at all five measurement frequencies. Although the radiosonde scaling affects the magnitude of the results presented in Fig. 1, the trends and our conclusions are not affected.

TABLE II  
EFFECT OF A 2% INCREASE IN PWV ON SLOPE OF  $\Delta T_B$  VS.  $T_B$  REGRESSION

Model	22.235 GHz	23.035 GHz	23.835 GHz	26.235 GHz	30.0 GHz
R03	0.067	0.057	0.035	-0.0008	-0.021
$\Delta$ Slope	-0.015	-0.015	-0.017	-0.021	-0.024

Despite the improvement associated with the HITRAN half-width, the agreement between measured and modeled brightness temperatures is not perfect. This is most likely due to small differences in the details of the tipping curve calibration procedures implemented by ARM for the MWR [12] and those implemented by the MWRP manufacturer, which were unavailable to us. A comparison of brightness temperatures measured with the MWRP at 23.835 GHz and with the MWR at 23.8 GHz is presented in Fig. 2 for liquid-water-cloud-free sky conditions. The trend of the differences in Fig. 2 matches the trend at 23.835 GHz in Fig. 1. A statistical summary of this comparison for both MWR measurement frequencies is provided in Table 3. The root-

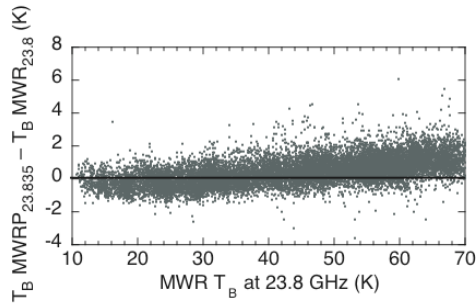


Fig. 2. Differences in measured brightness temperature  $T_B$  between the MWRP at 23.835 GHz and the collocated two-channel MWR at 23.8 GHz for liquid-water-cloud-free sky conditions.

TABLE III  
MWRP–MWR BRIGHTNESS TEMPERATURE DIFFERENCE STATISTICS FOR LIQUID-WATER-FREE SKY CONDITIONS DURING 2002

	23.835 – 23.8 GHz	30.0 – 31.4 GHz
Number of samples	13,711	13,711
Slope of $\Delta T_B$ vs. $T_B$ regression, K/K	0.030	0.070
Slope of $\Delta T_B$ vs. $T_B$ from model*, K/K	-0.009	0.048
Regression root-mean-square error, K	0.67	0.51
Mean $\Delta T_B$ (bias), K	0.48	0.32
Standard deviation $\Delta T_B$ , K	0.82	0.66

\*Rosenkranz [7].

mean-square errors of the MWRP–MWR regressions are less than the value of 0.71 K expected for radiometers with independent random errors of 0.5 K RMS. However, the slopes of the regressions are greater than predicted using the Rosenkranz model by 0.039 K/K at 23.835 GHz and by 0.022 K/K at 30.0 GHz, which are close to the slopes of the MWRP–model differences for the R03-H model at 23.835 GHz and 30.0 GHz in Table 1. This suggests the remaining differences in Fig. 1 reflect calibration details rather than spectroscopic issues.

For another view of the effect of the line half-width, in Fig. 3 we compare the ratio of brightness temperatures from absorption models [13], [14], and R03-H – further modified to be consistent with the MT\_CKD water vapor continuum formulation of Mlawer *et al.* [15] (hereinafter R03-H-CKD) – to results from R03 for low (1 cm) and high (4 cm) values of PWV. By comparing brightness temperature ratios, the results are not sensitive to the vertical distribution of water vapor in the selected radiosonde profiles. As the statistics in Table 4 demonstrate, the results presented in Fig. 3 are representative of the ensemble mean of a large number of sample profiles.

The ratios of the brightness temperatures measured with the MWRP to the R03 model values are also shown in Fig. 3 (open circles). Although the MWRP/R03 model ratios do not agree perfectly with any of the model/R03 ratios because of calibration differences between the MWRP and MWR, the trends nevertheless clearly support the smaller HITRAN width; the MWRP/R03 ratios are not constant with frequency and close to 1.0, as would be the case if the measurements supported the R03 model, and neither the 5% increase in the 22-GHz line strength proposed by Liebe *et al.* [13] nor the increased strength and width proposed by Cruz Pol *et al.* [14]

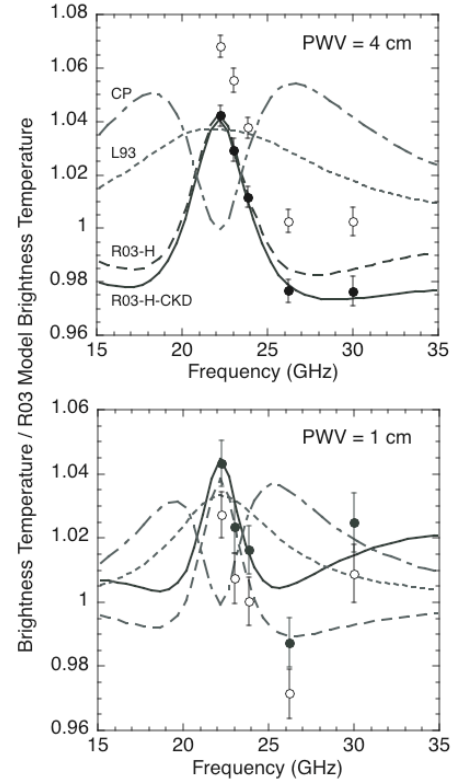


Fig. 3. Ratios of brightness temperature from modified versions of the Rosenkranz absorption model to results from the original model (R03) for 4 cm PWV (top) and 1 cm PWV (bottom): HITRAN half-width at 22 GHz (R03-H), HITRAN half-width and water vapor continuum adjustments consistent with MT\_CKD [15] (R03-H-CKD), 5% increase in 22-GHz line strength per Liebe *et al.* [13] (L93) and 6.4% increase in strength plus 6.6% increase in width per Cruz Pol *et al.* [14] (CP). Open circles are the mean ratio for measured  $T_B$  between 0.75 and 1.25 cm PWV and between 3.75 and 4.25 cm PWV; error bars are 99% confidence limits. Solid circles are the same as the open circles but are adjusted to agree with R03-H-CKD at 23.835 GHz.

TABLE IV  
R03-H-CKD TO R03 MODEL BRIGHTNESS TEMPERATURE RATIOS

	22.235 GHz	23.035 GHz	23.835 GHz	26.235 GHz	30.0 GHz
0.75 cm < PWV < 1.25 cm					
Samples	846	846	846	846	846
Mean Ratio	1.0441	1.0346	1.0196	1.0049	1.0134
Fig. 3 Ratio	1.0442	1.0324	1.0160	1.0046	1.0143
3.75 cm < PWV < 4.25 cm					
Samples	299	299	299	299	299
Mean Ratio	1.0402	1.0293	1.0106	0.9793	0.9749
Fig. 3 Ratio	1.0402	1.0302	1.0116	0.9787	0.9733

explain the trend of the data. To demonstrate this better, the ratio of the measurements was adjusted to agree with the R03-H-CKD ratio at 23.835 GHz, which is sensitive primarily to PWV, indicated in Fig. 3 by the solid circles. This is equivalent to rescaling the radiosonde data to achieve agreement between measured and modeled brightness temperatures at 23.835 GHz (i.e., a “physical retrieval” for PWV). This adjustment makes it clearer that the trend of the data supports the HITRAN half-width and also suggests that the MT\_CKD water vapor continuum formulation [15] is preferable.

Finally, ratios of the models and measurements to the modified Rosenkranz model using the HITRAN half-width R03-H are presented in Fig. 4, which clearly shows that the trend of the data supports the HITRAN width and MT\_CKD water vapor continuum formulation.

### III. CORRECTED TEMPERATURE AND WATER VAPOR RETRIEVALS

To quantify the effect of the HITRAN half-width on the profile retrievals, *a priori* statistical retrievals of temperature and water vapor profiles based on R03-H were developed for three-month periods (spring, summer, fall, and winter) by using 9041 radiosonde soundings launched from the SGP central facility in 1994–2000. These retrievals were applied to brightness temperatures measured with the MWRP at the SGP in July 2001–September 2002. Differences were calculated between the retrieved profiles of temperature and water vapor and those measured by 955 co-temporal (unscaled) Vaisala RS-90 radiosonde soundings. Unscaled soundings were used because we seek to quantify the retrieval performance relative to the RS-90 radiosondes, which the manufacturer claims have reduced or eliminated any dry bias [16]. Recent comparisons of RS-90 sondes with RS-80 sondes and other in situ sensors support this claim [17]. The mean (bias) and standard deviation of these differences are presented in Fig. 5, along with a comparison of the original neural network retrievals [4], which were based on R03. The results in Fig. 5 are for all (non-precipitating) sky conditions; results for liquid-water-cloud-free conditions alone are nearly identical.

The bias in the retrieved water vapor profiles in the lower and middle troposphere was substantially reduced with the new statistical retrieval based on R03-H. The standard deviation was slightly reduced. The large temperature bias in the upper troposphere was also substantially reduced with the new retrieval because the upper tropospheric temperature retrievals are dominated by the brightness temperatures at 51.25 and 52.28 GHz, which have significant contributions from water vapor and therefore are sensitive to errors in the water vapor absorption model. Because statistical and neural network retrievals for temperature and water vapor density profiles have been demonstrated to produce nearly identical results [4] when based on the same absorption model, these improvements can be entirely attributed to the effect of the HITRAN half-width.

Fig. 5 also presents calculations of the vertical resolution of the temperature and water vapor retrievals and the

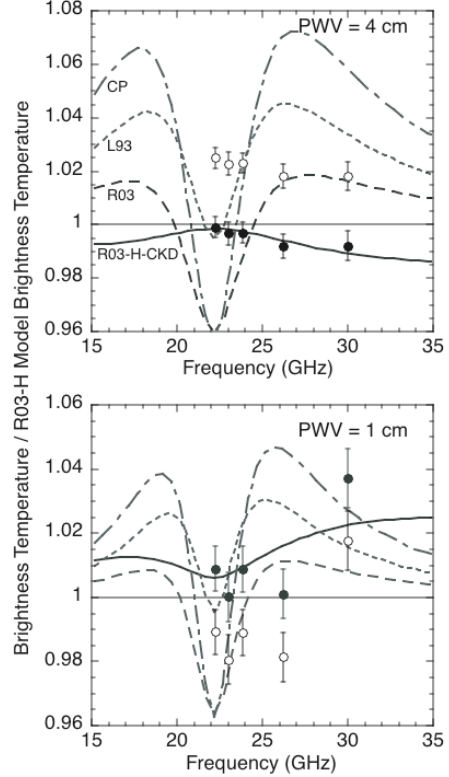


Fig. 4. Same as for Fig. 3 except the ratios are relative to the modified Rosenkranz model using the HITRAN half-width, R03-H.

improvement in resolution, particularly for water vapor, due to the HITRAN half-width. The vertical resolution of the retrieved temperature and water vapor profiles from the MWRP was determined by following [18], with the inter-level error covariance  $C(z_0, z)$  defined as

$$C(z_0, z) = \frac{\sum [Y(z_0) - Y_{sonde}(z_0)][Y(z) - Y_{sonde}(z)]}{\sqrt{\sum [Y(z_0) - Y_{sonde}(z_0)]^2 \sum [Y(z) - Y_{sonde}(z)]^2}} \quad (1)$$

Here  $z_0$  is the height for which the resolution is to be determined,  $Y$  is the retrieved temperature or water vapor,  $Y_{sonde}$  is the value measured by the radiosonde, and the summations are over all profiles in the ensemble. Noting that  $C(z_0, z_0) = 1$ , the resolution at  $z_0$  is defined as the distance between the heights  $z$  above and below  $z_0$ , where  $C = 0.5$ . This is the method used by [18] to calculate the vertical resolution of temperature and water vapor profiles derived from the ground-based Atmospherically Emitted Radiance Interferometer (AERI) spectrometer, which measures the infrared spectrum from  $500\text{--}3300\text{ cm}^{-1}$  ( $3\text{--}20\text{ }\mu\text{m}$ ) at  $1.0\text{ cm}^{-1}$  intervals, and also by [6] in an analysis of the MWRP neural network retrievals.

### IV. COMBINING MWRP AND GOES-8

To investigate the advantages of combining the MWRP with satellite-based sounders, we combined temperature and

water vapor profiles retrieved independently from the MWRP and the Geostationary Operational Environmental Satellite (GOES-8) sounder, which has 18 thermal infrared channels (ARM product spgg8profC1.a1) by using the inverse covariance weighting technique:

$$Y(z) = \frac{Y_1(z)\sigma_1^{-2}(z) + Y_2(z)\sigma_2^{-2}(z)}{\sigma_1^{-2}(z) + \sigma_2^{-2}(z)} \quad (2)$$

Here  $Y$  is the temperature or water vapor density profile,  $z$  is the altitude, subscripts 1 and 2 indicate the two independent measurements of  $Y$  to be combined, and  $\sigma^2$  is the error covariance, taken to be the square of the standard deviation of the difference between the retrieved profiles and collocated radiosonde soundings.

The results of the inverse covariance weighting are presented in Fig. 6, along with results from the combined GOES+AERI retrieval (ARM product spgaeriprofC1.c1) for reference. For temperature, bias of the combined system was reduced relative to that of the separate retrievals below 1 km. Above 1 km, the GOES retrieval dominates because of its significantly lower standard deviation, so the combined bias

tends toward the GOES-only bias. The vertical temperature resolution of the combined system was also improved relative to that of the separate systems. For water vapor, the benefit of the combination is not as dramatic because the standard deviations of the GOES retrieval errors are greater than or equal to the MWRP retrieval error standard deviation below 4 km. Above 4 km the vertical resolution did benefit noticeably. One limitation of the combined MWRP+GOES profiles (which is also applicable to the AERI+GOES retrievals) is that the infrared systems (GOES and AERI) are restricted to clear-sky conditions.

## V. MULTI-ANGLE RETRIEVALS

Although the retrievals described above use only zenith-pointing brightness temperature measurements, the vertical resolution of profile retrievals for passive radiometers can be improved by incorporating off-zenith measurements [19], [20]. To investigate this avenue, we developed statistical retrievals for temperature and water vapor density using brightness temperature measurements at an elevation angle of  $15^\circ$  (arbitrarily selected) in addition to zenith. This multiple-angle retrieval was evaluated by applying it to simulated brightness temperature measurements computed by adding 0.5

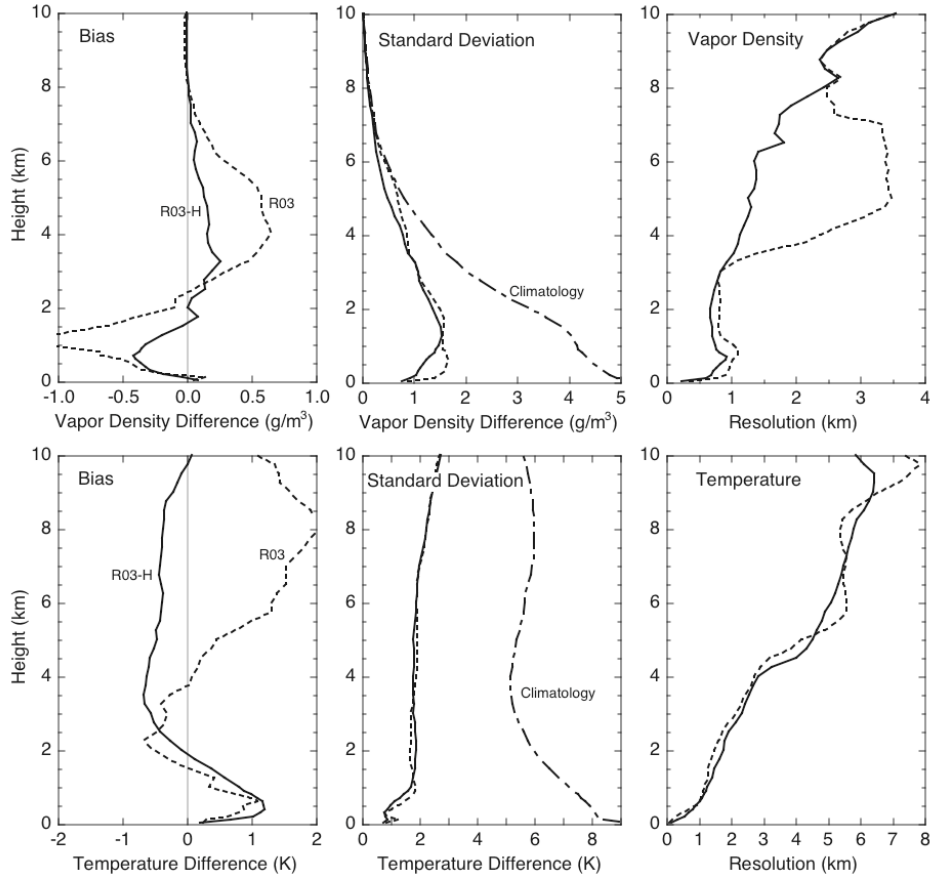


Fig. 5. Mean (bias) and standard deviation of the MWRP-radiosonde differences in the water vapor and temperature profiles for the original neural network retrievals (dashed) based on the Rosenkranz absorption model [7] (R03) and the new statistical retrievals (solid) based on the modified Rosenkranz model with the HITRAN [11] value for the half-width of the 22-GHz water line (R03-H) for non-precipitating (clear and cloudy) conditions. The standard deviation of the ensemble of radiosonde soundings about the mean of the ensemble ("Climatology") is provided for reference. The vertical resolutions of the original (dashed) and new (solid) water vapor and temperature retrievals are also shown.

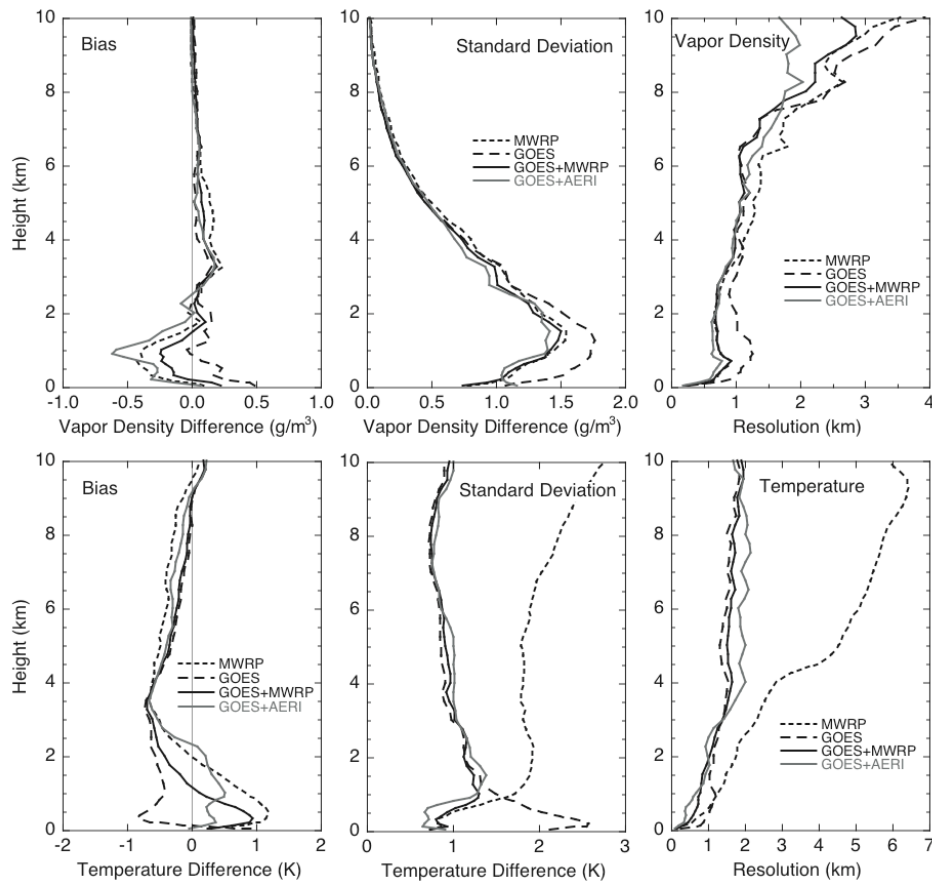


Fig. 6. Mean (bias) and standard deviation of the retrieval-radiosonde differences for water vapor and temperature profiles derived from the MWRP alone (short dash), GOES-8 sounder alone (long dash), GOES+MWRP (solid), and GOES+AERI (gray). Vertical resolution is also shown for water vapor and temperature profiles. Vertical resolution is defined as the distance between the heights where the inter-level error covariance for each level falls to 0.5.

K root-mean-square noise to model-calculated brightness temperatures and then computing the inter-level error covariances between the retrieved profiles and the input radiosonde profiles. The results (Fig. 7) suggest that improved resolution would be achieved in the water vapor density profile but not in the temperature profile. This is because the water vapor absorption at 22.235 GHz is relatively weak

compared with the oxygen absorption at 60 GHz; consequently the weighting functions for water vapor are broader than for temperature near the ground. Measurements at a  $15^\circ$  elevation angle sharpen the water vapor weighting functions much more than those for temperature. This results in noticeable improvement in the resolution for water vapor but not temperature at this elevation angle. Measurements at lower elevation angles may be required to improve the resolution of the temperature profile. A systematic study of the optimal frequency-angle combinations for each retrieval height is necessary.

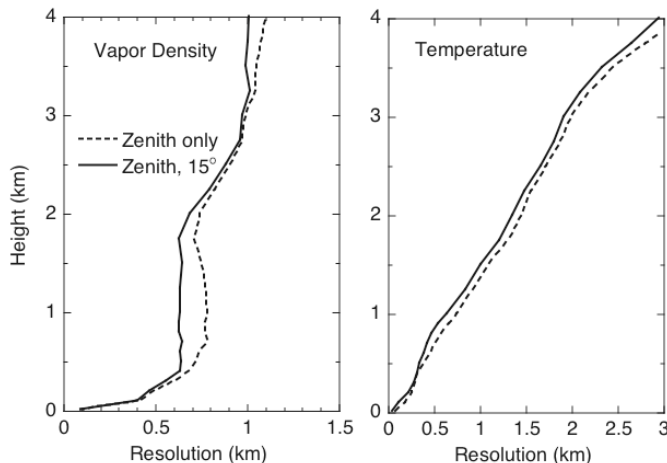


Fig. 7. Resolution of retrieved temperature and water vapor profiles for simulated measurements in the zenith only (dashed), and in the zenith and  $15^\circ$  elevation angle (solid).

## VI. CONCLUSION

Biases in retrieved temperature and water vapor profiles have been attributed to the half-width of the 22-GHz water vapor line used in the Rosenkranz absorption model, which is shown to be 5% too large. Retrievals based on the value for the half-width in the HITRAN database exhibited a temperature bias of less than 1 K and a water vapor bias of less than  $0.5 \text{ g/m}^3$ . The reduced line half-width also significantly improved the vertical resolution of the water vapor retrievals. Combining the ground-based MWRP retrievals with those from the GOES-8 sounder dramatically improved the temperature resolution and standard deviation in

the upper troposphere. Incorporating off-zenith brightness temperature measurements at 15° elevation into the retrievals improved water vapor profile resolution, suggesting that further study of the optimal combination of angles and frequencies for each height in the retrieval is warranted.

- [20] E. R. Westwater, Y. Han, and F. Solheim, "Resolution and accuracy of a multi-frequency scanning radiometer for temperature profiling," in *Microwave Radiometry and Remote Sensing of the Earth's Surface and Atmosphere*, P. Pampaloni, S. Paloscia, Eds., Zeist, The Netherlands: VSP Press, 2000, pp. 129-135.

## REFERENCES

- [1] F. S. Solheim, J. R. Godwin, and R. Ware, "Passive, ground-based remote sensing of temperature, water vapor, and cloud liquid profiles by a frequency-synthesized microwave radiometer," *Meteorologische Zeitschrift*, vol. 7, pp. 370-376, 1998.
- [2] S. Ghan, D. Randall, K.-M. Xu, R. Cederwall, D. Cripe, J. Hack, S. Iacobellis, S. Klein, S. Krueger, U. Lohmann, J. Pedretti, A. Robock, L. Rotstain, R. Somerville, G. Stenchikov, Y. Sud, G. Walker, S. Xie, J. Yio, and M. Zhang, "A comparison of single column model simulations of summertime midlatitude continental convection," *J. Geophys. Res.*, vol. 105, pp. 2091-2024, 2000.
- [3] J. C. Liljegren, "Evaluation of a new multi-frequency microwave radiometer for measuring the vertical distribution of temperature, water vapor, and cloud liquid water," unpublished.
- [4] F. S. Solheim, J. R. Godwin, E. R. Westwater, Y. Han, S. J. Keihm, K. Marsh, and R. Ware, "Radiometric profiling of temperature, water vapor, and cloud liquid water using various inversion methods," *Radio Sci.*, vol. 33, pp. 393-404, 1998.
- [5] P. Rosenkranz, "Water vapor continuum absorption: A comparison of measurements and models," *Radio Sci.*, vol. 33, pp. 919-928, 1998.
- [6] J. Gueldner and D. Spaenkuch, "Remote sensing of the thermodynamic state of the atmospheric boundary layer by microwave radiometry," *J. Atmos. and Ocean. Tech.*, vol. 18, pp. 925-933, 2001.
- [7] P. Rosenkranz, private communication, August 2003.
- [8] H. J. Liebe and D. H. Layton, "Millimeter-wave properties of the atmosphere: Laboratory studies and propagation modeling," NTIA Institute for Telecommunication Sciences, Boulder, CO, Report 87-224, 1987.
- [9] S. A. Clough, Y. Beers, G. P. Klein, and L. S. Rothman, "Dipole moment of water from Stark measurements of H<sub>2</sub>O, HDO, and D<sub>2</sub>O," *J. Chem. Phys.*, vol. 59, pp. 2254-2259, 1973.
- [10] H. J. Liebe and T. A. Dillon, "Accurate foreign-gas-broadening parameters of the 22-GHz H<sub>2</sub>O line from refraction spectroscopy," *J. Chem. Phys.*, vol. 50, pp. 727-732, 1969.
- [11] L. S. Rothman and co-authors, "The HITRAN molecular database: Editions of 1991 and 1992," *J. Quant. Spectrosc. Radiat. Transfer*, vol. 48, pp. 469-507, 1992.
- [12] J. C. Liljegren, "Automatic self-calibration of ARM microwave radiometers," in *Microwave Radiometry and Remote Sensing of the Earth's Surface and Atmosphere*, P. Pampaloni, S. Paloscia, Eds., Zeist, The Netherlands: VSP Press, 2000, pp. 433-443.
- [13] H. J. Liebe, G. A. Hufford, and M. G. Cotton, "Propagation modeling of moist air and suspended water/ice particle at frequencies below 1000 GHz," in *AGARD Conf. Proc.*, no. 542, May 1993, pp. 3.1-3.10.
- [14] S. L. Cruz Pol, C. S. Ruf, and S. J. Keihm, "Improved 20- to 32-GHz atmospheric absorption model," *Radio Sci.*, vol. 33, pp. 1319-1333, 1998.
- [15] E. J. Mlawer, S. A. Clough, D. C. Tobin, "The MT\_CKD water vapor continuum: a revised perspective including collision induced effects," Presented at the *Atmospheric Science from Space using Fourier Transform Spectrometry (ASSFTS) Workshop*, Bad Wildbad (Black Forest), Germany, 8-10 October 2003.
- [16] A. Paukkunen, V. Antikainen, and H. Jauhiainen, "Accuracy and performance of the new Vaisala RS90 radiosonde in operational use," in *Proc. 11<sup>th</sup> Symp. Meteorological Observations and Instrumentation*, Albuquerque, New Mexico, 14-18 January 2001, pp. 98-103.
- [17] A. K. Vance, J. P. Taylor, T. J. Hewison, and J. Elms, "Comparison of in situ humidity data from aircraft, dropsonde, and radiosonde," *J. Atmos. Ocean. Tech.*, vol. 21, pp. 921-932, 2004.
- [18] W. L. Smith, W. F. Feltz, R. O. Knuteson, H. R. Revercomb, H. B. Howell, and H. H. Wolf, "The retrieval of planetary boundary layer structure using ground-based infrared spectral radiance measurements," *J. Atmos. Ocean. Tech.*, vol. 16, pp. 323-333, 1999.
- [19] B. L. Gary, "Passive microwave temperature profiler," report JPL-D-5484, Jet Propulsion Laboratory, California Institute of Technology, Pasadena, CA, 1988.